

## Effect of Large-Amplitude Vibrations on the Thermodynamics of Malondialdehyde

Alfonso Niño\* and Camelia Muñoz-Caro

Grupo de Química Computacional, E.U Informática de Ciudad Real, Universidad de Castilla-La Mancha, Ronda de Calatrava 5, 13071 Ciudad Real, Spain

Received: July 21, 1997; In Final Form: November 12, 1997

A study of the effect of large-amplitude vibrations on the thermodynamic properties of malondialdehyde is presented. By using ab initio methodology at the MP2(FC)/6-311G(d,p) level, the internal rotation of the two aldehydic groups is analyzed. Two maxima are localized on the two-dimensional potential surface, and the global minimum is found in a  $C_1$  conformation. The highest maximum appears because of steric hindrance between the oxygens, whereas the second maximum is due to steric hindrance between the hydrogens of the two aldehydic groups. After determination of the nonrigid group of the molecule, we obtain kinetic and potential functions adapted to the  $a_1$  representation. With these functions, the two-dimensional vibrational Hamiltonian is solved variationally, and the torsional energy levels are calculated for the first time. The fundamental frequencies of vibration for the two torsional modes are found to be 48.35 and 87.01  $\text{cm}^{-1}$ . The effect of nonrigidity in the thermodynamic properties of malondialdehyde is determined by comparison of nonrigid and harmonic results. In the nonrigid case, it is found that the increase of the density of states affects mainly the value of the partition function, whereas its temperature derivative is almost constant.

### Introduction

Malondialdehyde is the simplest  $\beta$ -dicarbonyl compound. It is an interesting molecule from a biological point of view since it is one of the most significant products of metabolic or deteriorative lipid damage. Its formation during food processing and storage is used in quality control. In addition, its ability to react with  $-\text{NH}_2$  groups has carcinogenic and mutagenic interest because of the possible reaction with free amino acids, proteins, nucleic acids, and amino phospholipids. The different biological roles played by malondialdehyde have been reviewed by Aubourg.<sup>1</sup>

Malondialdehyde is also the prototype of the keto–enol interconversion and, in the enol form, the prototype of intramolecular hydrogen bonding and proton transfer. The most stable tautomer, enol, has been the subject of many theoretical studies dealing mainly with the problem of proton transfer.<sup>2–5</sup> In contrast, very few theoretical studies have been carried out on the keto form and those mainly involving some aspects of the conformational preferences of this tautomer.<sup>6–8</sup> The existence of large-amplitude vibrations in both tautomeric forms makes malondialdehyde well-suited for analyzing quantitatively the effect of soft vibrations on the thermodynamics of the keto–enol interconversion, especially the entropic variation. This is an aspect of the calculation of free energies in nonrigid molecules, a topic of interest for the modeling of biological systems.<sup>9</sup>

In the keto form the two aldehydic groups rotate against the CCC frame simultaneously, producing a pair of coupled large-amplitude vibrations. The result is a stack of torsional energy levels very different from the predictions of the usual harmonic approach. These large-amplitude vibrations have low-frequency energy levels, which appear as negative exponents in the partition function. Thus, the thermodynamics of the keto tautomer is especially influenced by these vibration modes. However, the usual model applied to the prediction of thermodynamic properties is the harmonic one, which gives a very

different pattern of energy levels. Despite this, the harmonic approach is widely employed, being easily applied with standard quantum-mechanical packages.<sup>10</sup> On the other hand, the Pitzer method<sup>11</sup> can enhance the results, but it does not consider the dependence of the kinetic terms on the large-amplitude coordinates. In addition, this method uses a too restrictive expression for the potential energy.

In this work, we start a theoretical study of the effect of large-amplitude vibrations on the keto–enol tautomerism. Thus, we begin analyzing the effect of large-amplitude vibrations in the thermodynamic properties of keto malondialdehyde. For this tautomer, we develop a two-dimensional vibrational model for the simultaneous torsion of the keto groups. The model accounts explicitly for the kinetic and potential coupling between both torsional modes. In addition, the dependence of the kinetic terms on the torsional coordinates is also considered. By developing analytic forms for the kinetic terms and the potential function, the torsional energy levels are calculated for the first time and introduced into the partition function. The effect of the nonrigidity of malondialdehyde on its thermodynamic properties is accounted for by comparison with the predictions of the harmonic approach. The origin of the discrepancy is analyzed.

### Theory

For the treatment of our two large-amplitude vibrations we will use the pure vibrational Hamiltonian,<sup>12</sup>

$$\hat{H} = \sum_i \sum_{j>i}^2 \left( -B_{ij} \frac{\partial^2}{\partial \theta_i \partial \theta_j} - \frac{\partial B_{ij}}{\partial \theta_i} \frac{\partial}{\partial \theta_j} \right) + V(\theta_1, \theta_2) \quad (1)$$

where  $B_{ij}$  are the kinetic terms,  $V$  is the potential, and  $\theta_1$  and  $\theta_2$  are the torsional coordinates. Equation 1 accounts for the noncommutability of the momentum operator and the  $B_{ij}$  terms. The  $B$  kinetic terms are obtained as  $-\hbar^2 g_{ij}/2$ , where  $g_{ij}$  are the

last  $2 \times 2$  elements of the rotational–vibrational  $\mathbf{G}$  matrix.<sup>12</sup> For our periodic two-dimensional problem, the kinetic terms and the potential will be expanded in a double Fourier series,

$$B_{ij} = \sum_{m=0} (a_{ij,m} \sin(m\theta_1) + b_{ij,m} \cos(m\theta_1)) \sum_{n=0} (c_{ij,n} \sin(n\theta_2) + d_{ij,n} \cos(n\theta_2))$$

$$V = \sum_{m=0} (e_m \sin(m\theta_1) + f_m \cos(m\theta_1)) \sum_{n=0} (g_n \sin(n\theta_2) + h_n \cos(n\theta_2)) \quad (2)$$

To account for the correct symmetry properties, these expansions must be adapted to the totally symmetric representation of the nonrigid group of the molecule. The Hamiltonian, eq 1, will be variationally solved in the free rotor basis.<sup>13</sup>

After calculation of the torsional energy levels, the thermodynamic properties of malondialdehyde will be statistically calculated from the partition function. Thus,

$$q = q_t q_r \prod_i^{3N-8} \exp[-\nu_0(i)/2kT] / (1 - \exp[-\nu_0(i)/kT]) \times \sum_j^{\infty} \exp[-\epsilon_j/kT] \quad (3)$$

with  $q_t$  and  $q_r$  being the translational and rotational partition functions,

$$q_t = (2\pi M k T / h^2)^{3/2} V$$

$$q_r = (\pi^{1/2} / \sigma) [(kT)^3 / (ABC)]^{1/2} \quad (4)$$

Here,  $M$  is the total mass,  $k$  the Boltzmann constant,  $h$  the Planck constant,  $T$  the absolute temperature,  $V$  the volume, and  $\sigma$  the symmetry number, i.e., the order of the rotational group of the molecule, and  $A, B, C$  are the rotational constants. In eq 3 the product runs on the harmonic vibrations and the summation corresponds to the vibrational levels for the two large-amplitude modes. The thermodynamic properties are calculated with the usual statistical formulas,<sup>14</sup>

$$G = -RT \ln Q + RTV(\partial \ln Q / \partial V)_T$$

$$H = RT^2(\partial \ln Q / \partial T)_V + RTV(\partial \ln Q / \partial V)_T$$

$$S = RT(\partial \ln Q / \partial T)_V + R \ln Q$$

$$U = RT^2(\partial \ln Q / \partial T)_V \quad (5)$$

### Computational Details

The molecular geometry, the normal mode analysis, and the kinetic and potential functions for malondialdehyde are obtained from ab initio results using the correlated, triple split plus polarization 6-311G(d,p) basis set. Correlation energy is accounted for at the MP2 (frozen core) level. All the calculations are carried out using the GAUSSIAN 94 package.<sup>10b</sup> The rotational–vibrational  $\mathbf{G}$  matrix and the kinetic terms for large amplitude vibrations are obtained using the KICO program,<sup>15</sup> whereas the vibrational energy levels are variationally calculated with NIVELON.<sup>16</sup> The thermodynamic properties in the

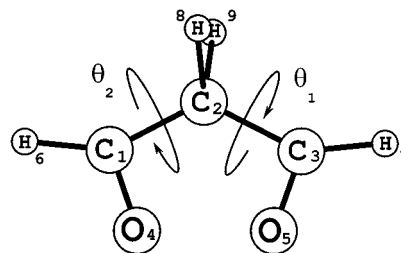


**Figure 1.** Numbering convention and origin conformation ( $\theta_1 = 0^\circ$ ,  $\theta_2 = 0^\circ$ ) for malondialdehyde.

**TABLE 1: Character Table for the  $G_4$  Group in Malondialdehyde**

$G_4$	$E$	(13)(45)(67)(89)	$E^*$	(13)(45)(67)(89)*
$A_1$	1	1	1	1
$A_2$	1	1	-1	-1
$B_1$	1	-1	-1	1
$B_2$	1	-1	1	-1

harmonic and nonrigid approaches have been calculated with the PARTI program.<sup>17</sup>

### Results and Discussion

The numbering convention used, the two torsional angles,  $\theta_1$  ( $O_5C_3C_2C_1$ ) and  $\theta_2$  ( $O_4C_1C_2C_3$ ), and the origin conformation ( $\theta_1 = 0^\circ$ ,  $\theta_2 = 0^\circ$ ) for malondialdehyde are shown in Figure 1. The nonrigid group for the double rotation of the keto groups is a  $G_4$  group with operations  $\{E, (13)(45)(67)(89), E^*, (13)(45)(67)(89)^*\}$ . These operations correspond to the identity, the simultaneous inversion and interchange of the torsional angles, the inversion of the torsional angles with respect to the CCC frame, and the interchange of  $\theta_1$  and  $\theta_2$ , respectively. This group is isomorphic to  $C_{2v}$ , and its character table is shown in Table 1.

A conformational analysis is performed on the  $\theta_1$  and  $\theta_2$  angles from  $0^\circ$  to  $180^\circ$  in increments of  $60^\circ$  (specific stationary points, such as global minimum and saddle points, are also determined). The positive sense of rotation is defined as clockwise when looking from  $C_1$  or  $C_3$  to  $C_2$ ; see Figure 1. At each point the molecular geometry is fully optimized. The global minimum is found in the  $C_1$  symmetry conformation  $\theta_1 = 2.63^\circ$ ,  $\theta_2 = -120.62^\circ$ . These data agree with the  $0^\circ$ ,  $120^\circ$  conformation obtained in ref 8, at the MP4(SDTQ)/6-31G(d,p)/6-31G(d,p) level, by keeping the first angle frozen at  $0^\circ$ . In the equilibrium conformation, the rotational constants are found:  $A = 0.4350 \text{ cm}^{-1}$ ,  $B = 0.1089 \text{ cm}^{-1}$ , and  $C = 0.0936 \text{ cm}^{-1}$ . At this point, a normal mode analysis is performed. The calculated harmonic frequencies are found (in  $\text{cm}^{-1}$ ): 67.89, 127.79, 245.63, 472.65, 656.41, 719.62, 866.35, 942.44, 1071.25, 1107.33, 1223.47, 1323.67, 1428.14, 1441.68, 1455.95, 1771.28, 1787.37, 2970.30, 2997.46, 3072.31, and 3141.09. An analysis of the normal coordinate composition shows that the two first modes correspond mainly to the internal rotation of the keto groups.

To derive a potential form for both internal rotations, the total energy data are fitted to a double Fourier expansion in  $\theta_1$  and  $\theta_2$  of symmetry adapted to the  $a_1$  representation of the  $G_4$  group. Thus, the potential function, eq 2, adopts the form

$$V = \sum_m \sum_n C_{mn} (\cos(m\theta_1) \cos(n\theta_2) + \cos(n\theta_1) \cos(m\theta_2)) + S_{mn} (\sin(m\theta_1) \sin(n\theta_2) + \sin(n\theta_1) \sin(m\theta_2)) \quad (6)$$

The resulting potential function is shown in Table 2 and the

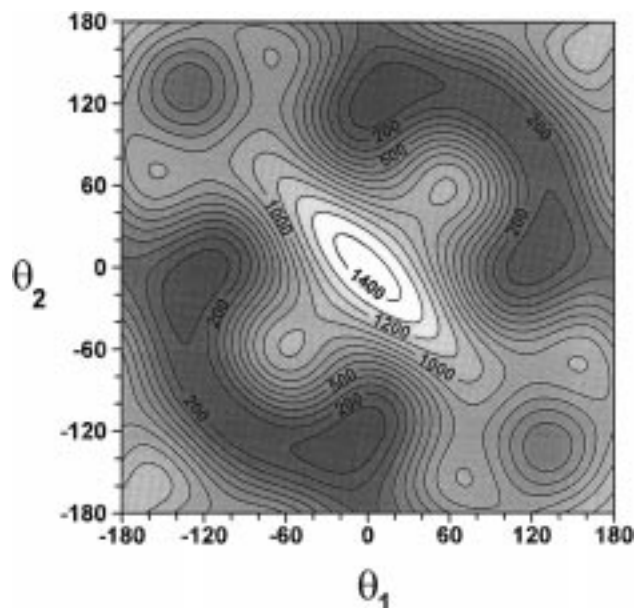


**Figure 2.** Potential energy surface for the simultaneous rotation of the keto groups in malondialdehyde. The interval between isopotential lines is  $200 \text{ cm}^{-1}$ . Darker zones represent low-energy zones.

**TABLE 2: Potential and Kinetic Terms Expansions for the Internal Rotation of the Keto Groups in Malondialdehyde: Expansion Terms in  $\text{cm}^{-1}$ ; Correlation and Standard Deviation Are Included**

term	V	$B_{\theta_1, \theta_1} = B_{\theta_2, \theta_2}$	$B_{\theta_1, \theta_2}$
$C_{00}$ (constant)	302.96	2.856	-0.522
$C_{10}$	55.33	0.478	-0.752
$C_{11}$	231.13	-0.082	0.001
$C_{20}$	28.89	0.442	-0.203
$C_{21}$	121.40	-0.134	-0.025
$C_{22}$	49.57	0.081	-0.032
$C_{30}$	-140.45	0.187	-0.091
$C_{32}$	67.03	-0.035	-0.028
$C_{33}$	8.22	-0.043	-0.002
$S_{11}$	-126.47	-0.036	-0.333
$S_{21}$	13.25	0.125	-0.079
$S_{22}$	76.61	0.081	-0.018
$S_{32}$	-113.26	-0.336	0.102
$S_{33}$	-13.03	0.253	-0.041
R	0.99985	0.99872	0.99999
$\sigma$ ( $\text{cm}^{-1}$ )	7.73	0.160	0.019

two-dimensional potential hypersurface in Figure 2. Bouma and Radom,<sup>6</sup> in a previous two-dimensional study performed using fixed distances and angles at the HF/STO-3G and HF/4-31G levels, found qualitatively similar results. However, our surface exhibits four equivalent global minima, owing to the  $G_4$  symmetry. A secondary minimum ( $104.84 \text{ cm}^{-1}$ ) is found at  $\theta_1 = 71.97^\circ$ ,  $\theta_2 = 124.27^\circ$ . The highest maximum ( $1431.46 \text{ cm}^{-1}$ ) is found in the  $\theta_1 = 0^\circ$ ,  $\theta_2 = 0^\circ$  (origin) conformation. This maximum appears as a consequence of steric hindrance between the two oxygens. For a similar reason, a smaller maximum ( $1019.31 \text{ cm}^{-1}$ ) appears at  $\theta_1 = 180^\circ$ ,  $\theta_2 = 180^\circ$  because of steric hindrance between the hydrogens. The minimum along the  $\theta_1 = \theta_2$  diagonal ( $C_2$  symmetry) is found to be  $106.82 \text{ cm}^{-1}$  at  $\theta_1 = \theta_2 = 101.78^\circ$ . This point is characterized as a first-order saddle point on the global  $3N-6$  dimensional hypersurface. These angle values are smaller than the  $\theta_1 = \theta_2 = 110^\circ$  and the  $\theta_1 = \theta_2 = 106.9^\circ$  results obtained by Mack<sup>8</sup> for  $C_2$  conformations in a one-dimensional study at the HF/4-31G and HF/6-31(d,p) levels, respectively. Another minimum ( $444.68 \text{ cm}^{-1}$ ) appears at  $\theta_1 = -\theta_2 = 124.55^\circ$ .

The kinetic terms for the rotation of the keto groups are

**TABLE 3: Torsional Energy Levels for the Double Rotation of the Keto Groups in Malondialdehyde; The First Energy Level Is Placed at  $94.42 \text{ cm}^{-1}$  of the Potential Well; Symmetry Referred to the  $G_4$  Nonrigid Group**

$\nu_1$	$\nu_2$	symm	$\nu$ ( $\text{cm}^{-1}$ )
0	0	$a_1$	0.00
		$b_2$	0.00
		$a_2$	0.05
		$b_1$	0.05
1	0	$a_1$	48.35
		$a_2$	48.36
		$b_2$	48.40
		$b_1$	48.40
2	0	$a_2$	68.01
		$a_1$	68.02
		$b_1$	76.34
		$b_2$	76.37
0	1	$a_2$	87.01
		$a_1$	87.09
		$b_1$	98.68
		$b_2$	98.82
1	1	$a_2$	114.45
		$a_1$	114.60
		$b_2$	129.81
		$b_1$	131.12

obtained from the rotational-vibrational  $\mathbf{G}$  matrix<sup>12</sup> at each point of the conformational analysis. We observed that the  $B_{\theta_1}$  and  $B_{\theta_2}$  pure kinetic terms vary from  $4.6$  to  $2.09 \text{ cm}^{-1}$  whereas the coupling,  $B_{\theta_1, \theta_2}$  term, changes from  $-2.79$  to  $-0.05 \text{ cm}^{-1}$ . These data show an important kinetic coupling between both motions. Similarly to the potential, the kinetic terms are expanded on an  $a_1$  symmetry adapted double Fourier expansion. The results are collected in Table 2. Using the potential and kinetic expansions, the Hamiltonian, eq 1, is variationally solved in the free rotor basis.<sup>13</sup> To factorize by symmetry the hamiltonian matrix, the following basis functions are used for each representation of the  $G_4$  group,

$$a_1: \cos(m\theta_1) \cos(n\theta_2) + \cos(n\theta_1) \cos(m\theta_2) \times \\ \sin(m\theta_1) \sin(n\theta_2) + \sin(n\theta_1) \sin(m\theta_2)$$

$$a_2: \cos(m\theta_1) \sin(n\theta_2) + \sin(n\theta_1) \cos(m\theta_2)$$

$$b_1: \cos(m\theta_1) \sin(n\theta_2) - \sin(n\theta_1) \cos(m\theta_2)$$

$$b_2: \cos(m\theta_1) \cos(n\theta_2) - \cos(n\theta_1) \cos(m\theta_2) \times \\ \sin(m\theta_1) \sin(n\theta_2) - \sin(n\theta_1) \sin(m\theta_2) \quad (7)$$

The obtained torsional energy levels are collected in Table 3. The pattern of energy levels is far from the stack of equally spaced energy levels predicted by the harmonic approach. The fundamental frequency of vibration is  $48.35 \text{ cm}^{-1}$  for the first mode and  $87.01 \text{ cm}^{-1}$  for the second. These data can be compared with the  $67.89$  and  $127.79 \text{ cm}^{-1}$  harmonic results; see above. As expected, our values are smaller since the harmonic frequencies computed at the Hartree-Fock and correlated levels overestimate the experimental results.<sup>18</sup>

The effect of nonrigidity in the thermodynamic properties of our molecule is accounted for by comparison with the harmonic results. Thus, internal energy,  $U$ , entropy,  $S$ , enthalpy,  $H$ , and Gibbs energy,  $G$ , are obtained for both the harmonic and the nonrigid models. In the harmonic case the canonical ensemble consists of a mixture of two enantiomers. These enantiomers correspond to torsional angles of  $\theta_1 = 2.63^\circ$ ,  $\theta_2 = -120.62^\circ$  and  $\theta_1 = 120.62^\circ$ ,  $\theta_2 = -2.63^\circ$ , respectively. Taking into account that the molecular partition function is the same for

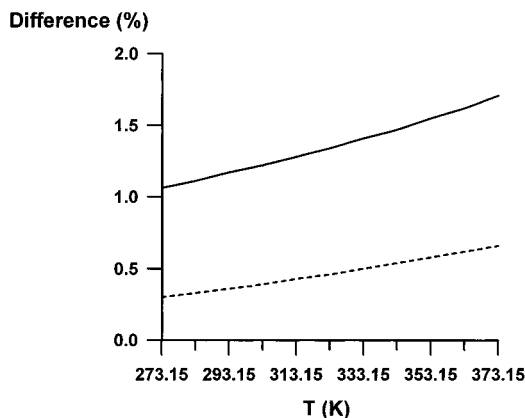


**Figure 3.** Difference between harmonic and nonrigid  $\ln Q$  (solid line) and  $(\partial \ln Q/\partial T)_v$  (dashed line) values as a function of temperature. The difference is calculated as  $100 \times (\text{harmonic value} - \text{nonrigid value})/(\text{nonrigid value})$ .

**TABLE 4: Thermodynamic Properties of Malondialdehyde Calculated with Harmonic and Nonrigid Models; Data Obtained at 298.15 K and a Pressure of 1 atm**

	case a <sup>a</sup>	case b <sup>b</sup>
$U$ (kJ/mol)	187.2	186.5
$S$ (J/(mol K))	319.4	320.6
$H$ (kJ/mol)	189.7	189.0
$G$ (kJ/mol)	94.5	93.4

<sup>a</sup> Harmonic results. <sup>b</sup> Nonrigid results.

both enantiomers, the canonical partition function is obtained as

$$Q = q^N / [(N/2)!]^2 \quad (8)$$

The nonrigid results are obtained with eq 3 using the torsional energy levels computed with the data of Table 2. Since the energy levels are very close, we introduced 400 of them in the direct summation of states. In the nonrigid case, for given values of the torsional angles we have four different isoenergetic conformers corresponding to  $(\theta_1, \theta_2)$ ,  $(\theta_2, \theta_1)$ ,  $(-\theta_1, -\theta_2)$ , and  $(-\theta_2, -\theta_1)$  angles; see Figure 2. These four conformers correspond to two sets of two elements  $\{(\theta_1, \theta_2), (\theta_2, \theta_1)\}$  and  $\{(-\theta_1, -\theta_2), (-\theta_2, -\theta_1)\}$ . Elements of different sets are enantiomeric forms, whereas elements of the same set are superimposable by a  $C_2$  rotation. This is a consequence of the existence of the (13)(45)(67)(89) operation in the nonrigid group, i.e., a  $C_2$  axis in the highest symmetry conformation. Thus, a symmetry number of 2 is used in the nonrigid model. Table 4 shows the results obtained at a temperature of 298.15 K and a pressure of 1 atm. When considering nonrigidity, it can be observed that the  $U$ ,  $H$ , and  $G$  values decrease, whereas  $S$  increases. The variation is similar in all the cases. As in

methanol,<sup>19</sup> we trace the origin of the difference between harmonic and nonrigid models to the behavior of  $\ln Q$  and  $(\partial \ln Q/\partial T)_v$ . Figure 3 shows that this difference is higher for  $\ln Q$  than for  $(\partial \ln Q/\partial T)_v$ . Both curves are almost parallel, although the  $\ln Q$  increases faster with temperature.

**Acknowledgment.** The authors would like to thank the DGICYT (Project No. PB93-0142-C03-03) and the Universidad de Castilla-La Mancha for financial support.

## References and Notes

- (1) Aubourg, S. P. *Int. J. Food Sci. Tech.* **1993**, *28*, 323.
- (2) (a) Shida, N.; Barbara, P. F.; Almlöf, J. E. *J. Chem. Phys.* **1989**, *91*, 4061. (b) Bosch, E.; Moreno, M.; Lluch, J. M.; Bertran, J. *J. Chem. Phys.* **1990**, *93*, 5685.
- (3) (a) Frisch, M. J.; Scheiner, A. C.; Schaefer, H. F., III; Binkley, J. S. *J. Chem. Phys.* **1985**, *82*, 4194. (b) Binkley, J. S.; Frisch, M. J.; Schaefer, H. F., III. *Chem. Phys. Lett.* **1986**, *126*, 1. (c) Latajka, Z.; Scheiner, S. *J. Phys. Chem.* **1992**, *96*, 9764. (d) Luth, K.; Scheiner, S. *Int. J. Quantum Chem. Quantum Chem. Symp.* **1993**, *27*, 419. (e) Luth, K.; Scheiner, S. *J. Phys. Chem.* **1994**, *98*, 3582. (f) Barone, V.; Adamo, C. *J. Chem. Phys.* **1996**, *105*, 11007.
- (4) Smedarchina, Z.; Siebrand, W.; Zgierski, M. *Z. J. Chem. Phys.* **1995**, *103*, 5326.
- (5) (a) Guo, Y.; Sewell, T. D.; Thompson, D. L. *Chem. Phys. Lett.* **1994**, *224*, 470. (b) Sewell, T. D.; Guo, Y.; Thompson, D. L. *J. Chem. Phys.* **1995**, *103*, 8557. (c) Bosch, E.; Moreno, M.; Lluch, J. M. *Chem. Phys.* **1992**, *159*, 99. (d) Ruf, A.; Miller, W. H. *J. Chem. Soc., Faraday Trans.* **1988**, *84*, 1523.
- (6) Bouma, W. J.; Radom, L. *Aust. J. Chem.* **1978**, *31*, 1649.
- (7) Buemi, G.; Gandolfo, C. *J. Chem. Soc., Faraday Trans.* **1989**, *85*, 215.
- (8) Mack, H.-G. *NATO ASI Ser., Ser. C*, **1993**, *410*, 535.
- (9) Leach, A. R. *Molecular Modelling. Principles and Applications*; Addison Wesley Longman Limited: U.K., 1996; Chapter 9.
- (10) (a) GAMESS: Schmidt, M. W.; Baldridge, K. K.; Boatz, J. A.; Elbert, S. T.; Gordon, M. S.; Jensen, J. H.; Koseki, S.; Matsunaga, N.; Nguyen, K. A.; Su, S.; Theresa, L. W.; Dupuis, M.; Montgomery, J. A., Jr. *J. Comput. Chem.* **1993**, *14*, 1347. (b) Frisch, M. J.; Trucks, G. W.; Schlegel, H. B.; Gill, P. M. W.; Johnson, B. G.; Robb, M. A.; Cheeseman, J. R.; Keith, T. A.; Petersson, G. A.; Montgomery, J. A.; Raghavachari, K.; Al-Laham, M. A.; Zakrzewski, V. G.; Ortiz, J. V.; Foresman, J. B.; Cioslowski, J.; Stefanov, B. B.; Nanayakkara, A.; Challacombe, M.; Peng, C. Y.; Ayala, P. Y.; Chen, W.; Wong, M. W.; Andres, J. L.; Replogle, E. S.; Gomperts, R.; Martin, R. L.; Fox, D. J.; Binkley, J. S.; Defrees, D. J.; Baker, J.; Stewart, J. P.; Head-Gordon, M.; Gonzalez, C.; Pople, J. A. *Gaussian 94* (Revision B.3); Gaussian, Inc.: Pittsburgh, PA, 1995.
- (11) (a) Pitzer, K. S.; Gwinn, W. D. *J. Chem. Phys.* **1942**, *10*, 428. (b) Pitzer, K. S. *J. Chem. Phys.* **1946**, *14*, 239. (c) Kilpatrick, J. E.; Pitzer, K. S. *J. Chem. Phys.* **1949**, *17*, 1064.
- (12) (a) Pickett, H. M. *J. Chem. Phys.* **1972**, *56*, 1715. (b) Harthcock, M. A.; Laane, J. *J. Phys. Chem.* **1985**, *89*, 4231. (c) Niño, A.; Muñoz-Caro, C. *Comput. Chem.* **1994**, *18*, 27.
- (13) Muñoz-Caro, C.; Niño, A.; Moule, D. C. *Chem. Phys.* **1994**, *186*, 221.
- (14) Lucas, K. *Applied Statistical Thermodynamics*; Springer-Verlag: Berlin, 1991.
- (15) Muñoz-Caro, C.; Niño, A. *QCPE Bull.* **1993**, *13*, 4.
- (16) Muñoz-Caro, C.; Niño, A. *QCPE Bull.* **1995**, *15*, 48.
- (17) (a) Niño, A.; Muñoz-Caro, C. *QCPE Bull.* **1997**, *17*, 1. (b) Niño, A.; Muñoz-Caro, C. *Comput. Chem.* **1997**, *21*, 143.
- (18) Pople, J. A.; Schlegel, H. B.; Krishnan, R.; Defrees, D. J.; Binkley, J. S.; Frisch, M. J.; Whiteside, R. A.; Hout, R. F.; Hehre, W. J. *Int. J. Quantum Chem.* **1981**, *15*, 269.
- (19) Muñoz-Caro, C.; Niño, A.; Senent, M. L. *Chem. Phys. Lett.* **1997**, *273*, 135.